

ON-AXIS 3D MICROSCOPE FOR X-RAY BEAMLINES AT NSLS-II

K. J. Gofron[†], J. Wlodek¹, Y.Q. Cai, NSLS-II, Brookhaven National Laboratory, Upton, NY, USA
¹also at Stony Brook University, Stony Brook, NY, USA

Abstract

A series of versatile on-axis X-ray microscopes with large working distances, high resolution and large magnification have been developed at NSLS-II [1,2]. These microscopes use reflective optics, which minimizes dispersion, and allows imaging from Ultraviolet (UV) [3] to Infrared (IR) with specifically chosen objective components (coatings, etc.). Additional customizations can be implemented to provide dual-view with high/low magnification [4], 3-D imaging, long working range, as well as ruby fluorescence measurement for high pressure samples. In this publication we discuss 3D imaging enhancement to on-axis microscopes.

INTRODUCTION

The National Synchrotron Light Source II (NSLS-II) on Long Island, NY, USA is a new synchrotron user facility constructed to provide extremely bright x-rays for a broad range of basic and applied research. A typical NSLS-II hard X-ray beamline achieves routinely submicron beam sizes. To facilitate optics alignment and optimization, as well as for sample monitoring and characterization, on-axis microscopes [1] have been developed at NSLS-II to provide online imaging capabilities with high spatial resolution around the sample area. Utilizing the imaging capability, for example, beam focus from focusing X-ray optics, such as KB-mirrors, can be visualized directly, providing instantaneous feedback during the optimization process, vastly improving the efficiency of characterization compared to the more traditional knife edge scans.

The details of the on-axis microscope as implemented at the Inelastic X-ray Scattering (IXS) 10-ID beamline are presented in Figures 1, and 2. The microscope is located downstream of the KB mirror system. Figure 1 (upper panel) illustrates the schematic of the optical layout, where the objective is folded from upstream using a right-angle mirror containing a hole for the X-ray beam to pass through (see Figure 2). Due to spatial constraint, such as the need of a sample cryostat, the microscope design at 10-ID incorporates an additional mirror in “periscope” geometry as shown in Figure 1 (lower panel).

The image of high pressure diamond anvil cell sample obtained using the on-axis microscope at 10-ID is shown in Figure 2 (lower panel). The cross-hair indicating the X-ray beam incidence position is injected into the image stream using the Overlay Plugin of areaDetector [5] EPICS application. The position of the cross-hair is determined by visualizing the X-ray beam using high-Z scintillator, such as CWO, placed at sample position [6].

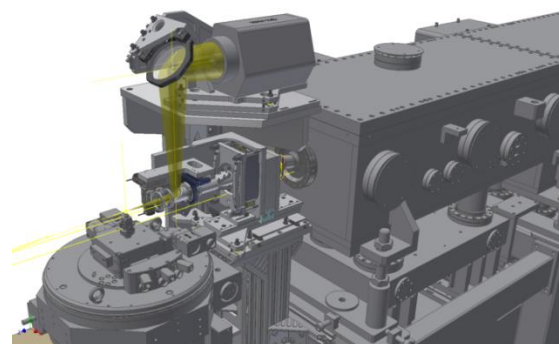
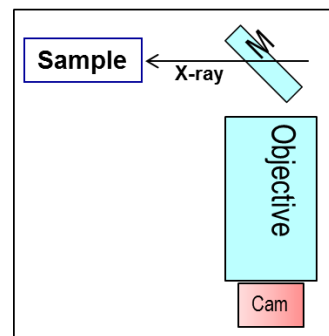


Figure 1: On-axis microscope schematics (upper panel), and the implementation at the IXS 10-ID beamline (lower panel).

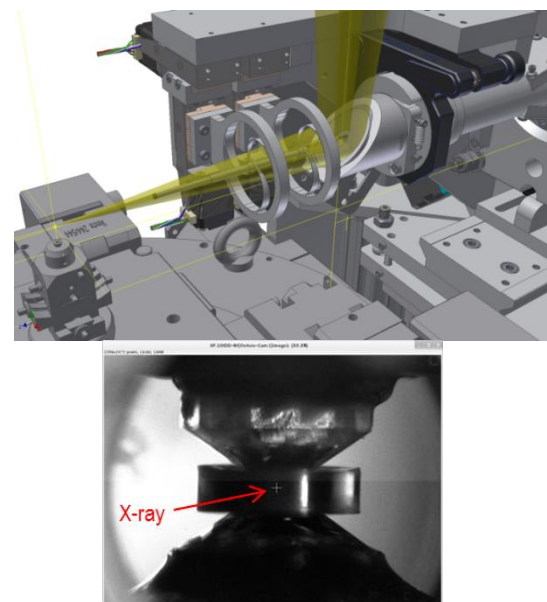


Figure 2: The on-axis microscope at 10ID with details near the sample area (upper panel), and image of a diamond anvil cell (DAC) sample (lower panel). The cross indicates the X-ray beam position.

The 10-ID on-axis microscope has a working distance of 600 mm and resolution of 3 μm . An incorporated

Content from this work may be used under the terms of the CC BY 3.0 licence (© 2017). Any distribution of this work must maintain attribution to the author(s), title of the work, publisher, and DOI.

[†] kgofron@bnl.gov

GT330 Prosilica PoE camera provides 6 mm x 4.5 mm field of view.

X-RAY EYE

The X-ray Eye microscope is a downstream version of the on-axis microscope that may be implemented with a right angle folding mirror when space is limited. The X-ray Eye allows very high precision X-ray beam characterization. The X-ray eye microscope consists of a scintillator, and conventional optical microscope. The microscope images the visible light generated by X-ray at the scintillator. The schematics of the optical layout and the actual 10-ID X-ray Eye microscope as built with a right angle folding mirror are shown in Figure 3.

Optics Layout

The X-ray eye microscope developed for the 10-ID beamline, shown in Figure 3, is adapted so the scintillator is exactly at the sample position. This allows optimization of the KB mirror optics shown in Figure 4, which illustrates the focusing of the VFM mirror, with the HFM mirror removed from the beam. The focus width of VFM X-ray beam is determined using right peak of the Figure 4 (lower panel).

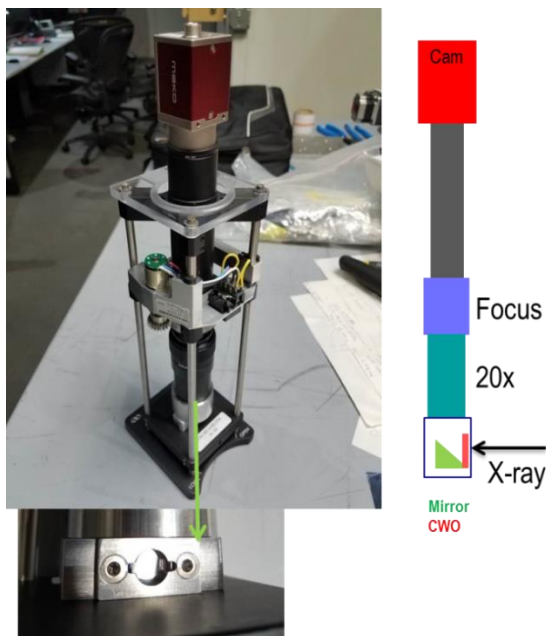


Figure 3: X-ray Eye microscope for beam characterization.

The left peak of Figure 4 (lower panel) is an optical artefact of using second surface mirror instead of first surface mirror in initial assembly of the microscope shown in Figure 3. The left optical reflection peak originated from the small wedge air gap between scintillator and the first surface of the 2nd surface mirror.

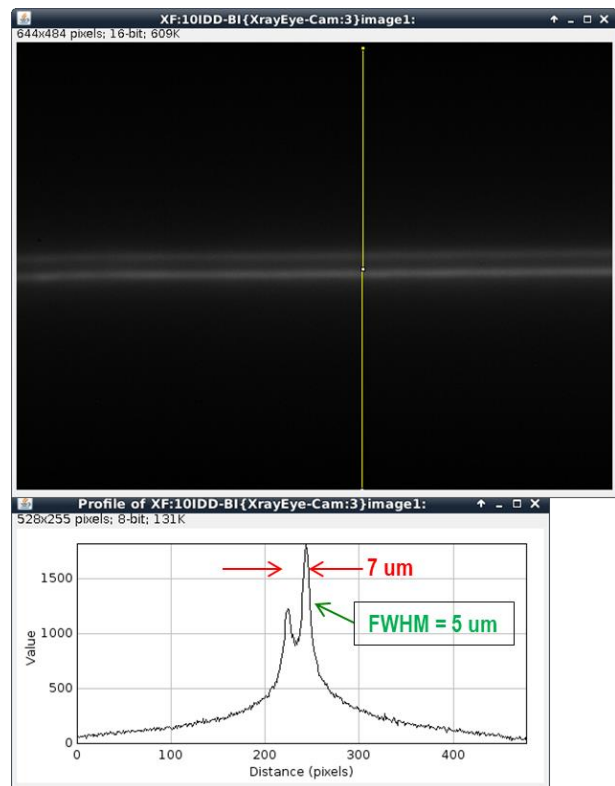


Figure 4: KB mirror alignment of the VFM mirror at 10-ID. The cross-section intensity of upper image is plotted in the lower image.

3D MICROSCOPE

Shallow Depth of Field (DoF) is a weakness in microscopy. The DoF is generally proportional to the resolution, and decreases for high magnification and large Numerical Aperture.

In this paper we will demonstrate that shallow depth of focus can be used to derive information about 3D nature of the object under study using Image Stacking technique. In Image Stacking the information about depth dimension is obtained by calibrated move of either objective, or the sample under study. We have used both, with successful results.

Image Stacking

Image Stacking, as shown in Figure 5, is the process by which a series of images of the same subject taken at different focal depths are combined in order to form one in-focus image. This process (which is also sometimes called focus stacking), can allow users to view samples with a greater level of detail without resorting to constantly adjusting the camera position or focus.

There are two primary methods to collect an image stack. The first is to move the camera itself, and the second is to change the focal depth of the camera. A sample is placed under a microscope or a high magnification camera such as the On-Axis camera at the Inelastic X-Ray Scattering (IXS) Beamline and the

Content from this work may be used under the terms of the CC BY 3.0 licence © 2017. Any distribution of this work must maintain attribution to the author(s), title of the work, publisher, and DOI.

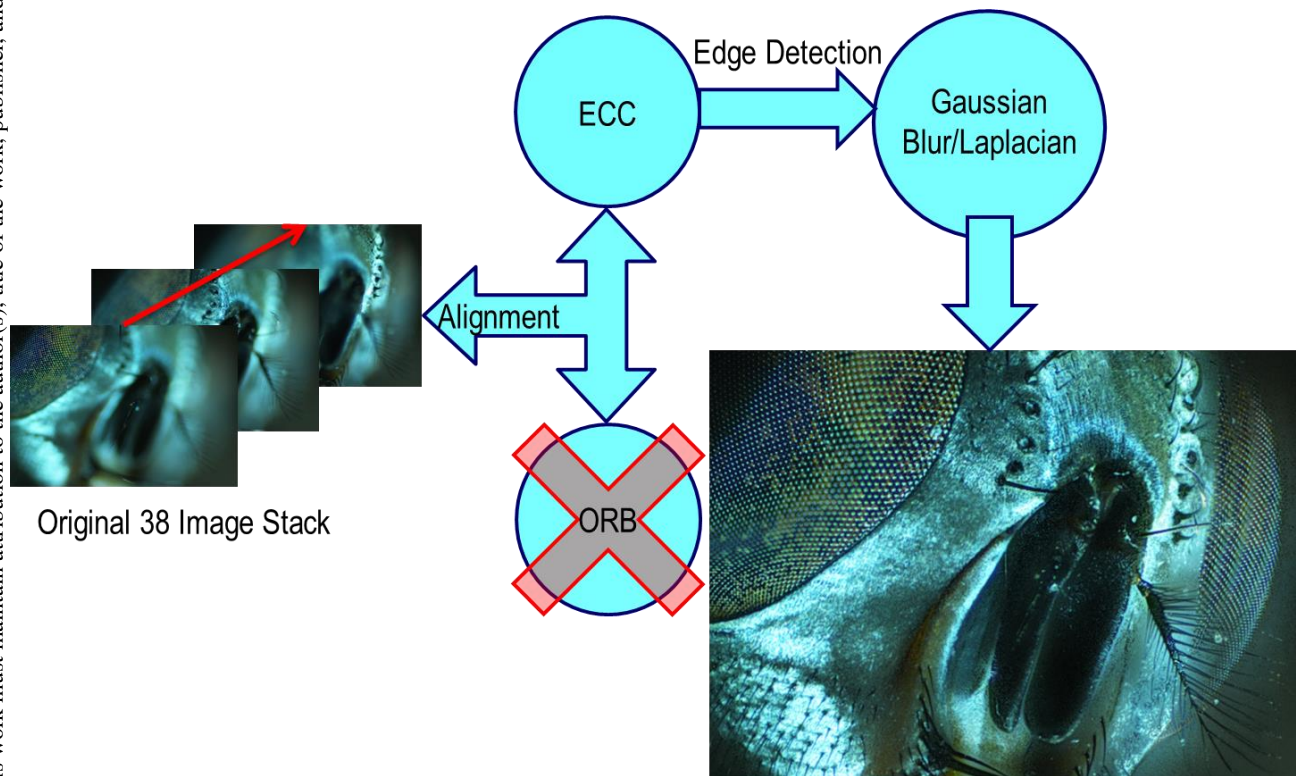


Figure 5: Image stacking methods that we used.

camera's focal depth is adjusted in such a way that there is at least one image per portion of the sample where the area is in focus. Once such a stack is collected for a chosen sample, it is run through a focal stacking algorithm, as discussed in details by J. Wlodek [7].

The first step of this algorithm involves image alignment. On most microscopes and cameras, changing the focal depth will cause either a shift of the subject in the view, a resizing of the subject, or both. As a result, in order to avoid an incorrect merging of the images in the later steps of the algorithm, image alignment is necessary. Two image alignment methods have been implemented: one uses the Oriented Fast and Rotated Brief (ORB) feature detector in conjunction with the Brute Force Matcher as implemented in the Open Computer Vision (OpenCV) library [8], while the other uses a Euclidean transfer (ECC) to find how to shift images until they are aligned. The ORB method unfortunately proved to be inadequate despite its speed, as a result of its dependence on finding matching key points in images, which was often hampered by the fact that large portions of each image in the stack were out of focus, and hence had no detectable key points. Thus the ORB alignment method often provided sub-par results. The ECC method on the other hand gave much better results and provided greater flexibility as well, with users being able to specify the degree of accuracy they wished the algorithm to run with, as well as a warp mode, as the Euclidean transfer allows for finding a translation, a rotation, an affine transform (rotation, translation, and scaling), or even a homography

(affine and tilt) between two images. This made the alignment algorithm very flexible in regards to the sample images.

Once the stack of images was aligned, the next step in the focus stacking algorithm was to run an edge detector over each image in the stack. This was accomplished by running a Gaussian blur matrix over each of the images, followed by Laplacian. This process assigned each pixel a "sharpness value", a value that represented the relative sharpness of that pixel in an image. The final step of the algorithm was to create an empty image of the same size as one of the input images, and fill it with the pixels with the highest sharpness values across all of the images in the stack. The output image is then saved to the host computer.

For the On-Axis camera at the IXS 10-ID beamline we demonstrated an implementation of the open source EPICS control system library to automate focus stack collection. The code requires the user to first find a start and end point for where the sample is in focus in order to avoid unnecessary photos in the stack, and the user is required to specify a number of images. The number cannot be too high, as overlapping in focus areas can cause problems for generating an accurate depth map, which can be used for three dimensional reconstruction, while a number too low will miss certain regions, which will lead to parts of the image remaining out of focus. The merged image in Figure 5 and Figure 6, have missed regions visible as superstructure bands of the horse fly right eye. Once the variables are inputted, the code splits

the distance between the start and end point into the specified number of subdivisions, automatically moves the motor to each of these points and takes a picture.

Once a stack is collected by the EPICS script, it is passed to the image stacking software, and is combined into one image. This image can be used by the staff of the IXS beamline to get a better view of their sample, and see all the detail without the need for constant time consuming adjustments to camera focus. An additional benefit of focus stacking is that it can provide scientists with images that were previously unattainable with such shallow depth of focus cameras, allowing for more detailed and compelling images to be obtained for presentations and publications.

In addition to the merged image, image stacking also allows for a form of 3D reconstruction, even with a single stationary camera, something that is not possible with photogrammetry or stereo reconstruction. To do this, as we constructed the merged image from the data found during the edge detection phase, we also constructed a depth map of all of the images. This process is explained in further detail by Michael Moeller in his paper "Variational Depth from Focus Reconstruction" [9]. Each image in the stack was assigned a grayscale value from 0 to 255, with the stack evenly spaced out across this range. At each pixel, when the sharpest pixel is chosen, the corresponding pixel in the depth map is set to the grayscale value assigned to the image that the merged pixel was taken. Once this entire depth map is constructed, it is smoothed to remove jagged edges in the three dimensional model.

After the stacking algorithm is completed and the depth map is generated, we used the OpenGL graphics library [10] to create our 3D models. The X and Y values of each pixel in the model corresponded directly to the X and Y pixel values of the merged image, while the Z, or height, value was derived from the product of the grayscale value of the depth map at said pixel, and a conversion factor that is determined by the ratio of micrometers to pixels as well as the change in focal depth. Once all of these values are computed, the model is drawn and can be rotated freely.

Both the depth map and three dimensional model provided by focus stacking with the On-Axis Microscope allow for a unique perspective on samples being studied, providing depth information that previously would have had to be manually calculated. It allows for faster analysis of data and samples, and allows for interesting showcases that can be used to demonstrate findings to others.

Imaging head of a Horse Fly We tested image stacking applications on a Horse Fly positioned under a 5x magnification microscope. We collected a stack of 38 images, which were combined to form one merged image. The difference we see in Figure 6 between one of the images taken from the stack and the merged image is striking, and effectively shows the benefit that such a

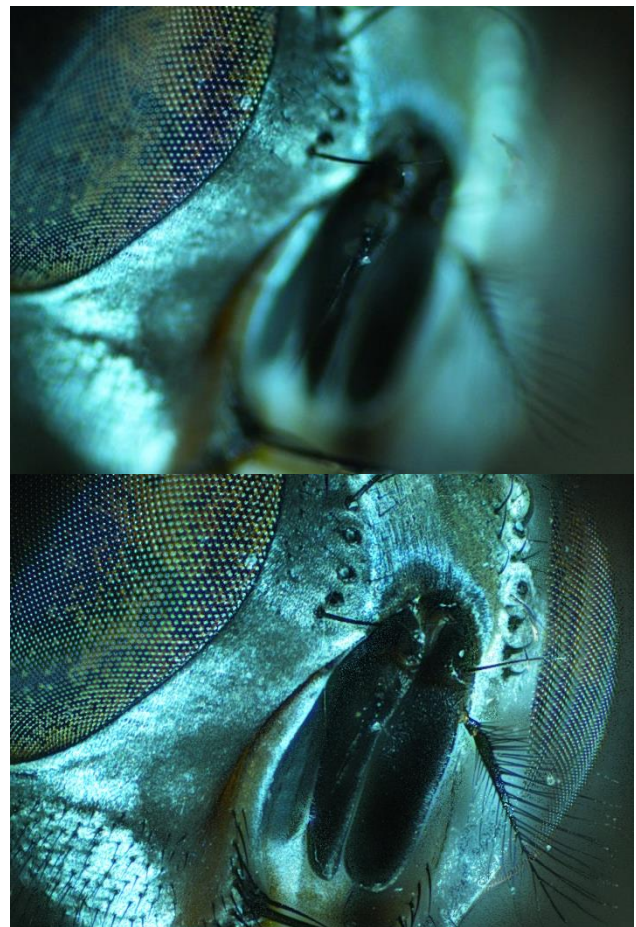


Figure 6: Single image from 5X microscope (upper panel), and one obtained from Image Stack (lower panel).

technique could provide if the user wishes to have a detailed single image of his or her subject.

Imaging a mineral As a way to test the system on a different kind of sample, we examined a mineral under the same 5x microscope as the fly, and once again utilized the image stacking techniques discussed earlier. Additionally, we deployed the 3D imaging application to this stack as well, and it provided some great results. Figure 7 shows the merged image and the depth map obtained from the mineral, and additionally a video of the mineral's three dimensional OpenGL model is available at: https://www.youtube.com/channel/UC-SfBpwDIuw41_r0qqYkZQ [11].

Imaging a beetle The image stacked results of a beetle obtained at 10-ID on-axis microscope are shown in the Figure 8 (upper panel). The lower panel of Figure 8 shows the depth map obtained from images. Using the depth map a 3D video of the beetle was produced [11].

Content from this work may be used under the terms of the CC BY 3.0 licence (© 2017). Any distribution of this work must maintain attribution to the author(s), title of the work, publisher, and DOI.

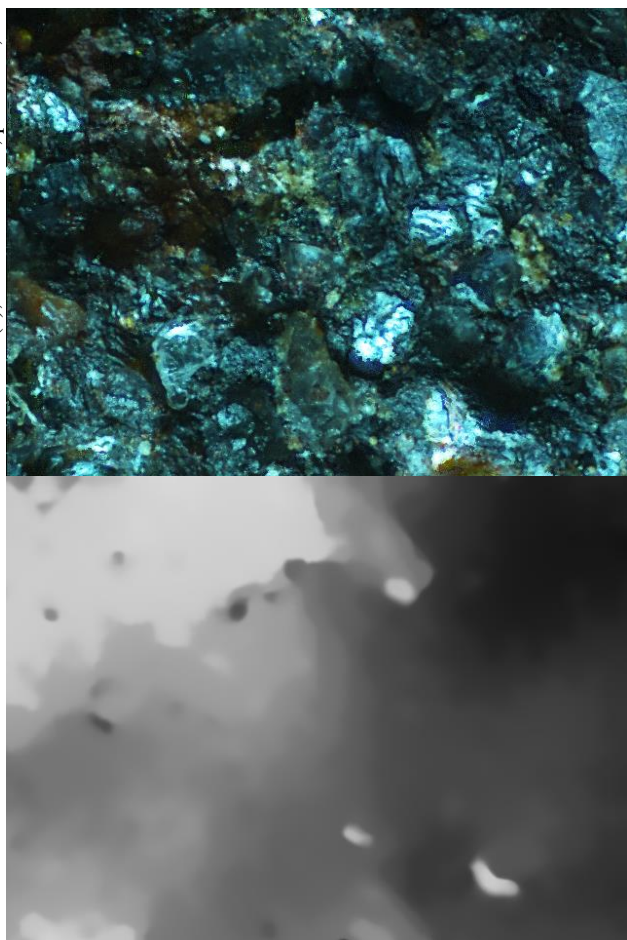


Figure 7: Image of a mineral (upper panel) and its depth map (lower panel).



Figure 8: Image of a beetle (upper panel) and depth map (lower panel).

CRYSTAL HARVESTING

We used the development of the 3D microscope to understand biological crystal harvesting using acoustic waves [12].

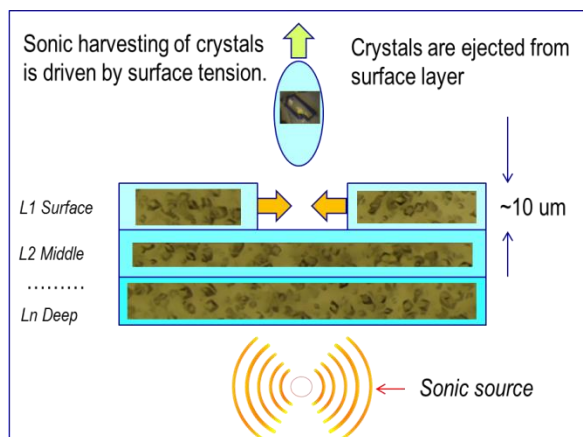


Figure 9: Acoustic harvesting of biological crystals.

In acoustic protein crystal harvesting, proteins are harvested by utilizing sonic pulses generated by a source underneath them. Each pulse is just strong enough to launch a crystal from the surface upwards. Prior to the application of the 3D Microscope techniques, the process immediately following crystal ejection was not understood. The accepted theory was that crystals were moved toward the top of the solution in a conical manner, funneling crystals that lay on the bottom of the liquid to the top. This has led to the fact that crystals are rarely grown in a Bingham solution (a solution that keeps crystals suspended rather than falling to the bottom of the well), because such a solution requires more work to maintain. The necessity of a Bingham solution was not considered important, because it was thought that crystals would be resupplied from the bottom of the drop after ejection. Despite this, users of the sonic machines have noted a drop off in the efficiency of crystal harvesting after several ejections. In order to solve this issue, we collected a stack of images of the drop at several points both before and after ejections, and constructed a depth map and a model at each point. Once these were constructed, we used optical flow to determine the distance that a set of roughly 30 crystals travelled in the drop, as well as measuring their height in the drop. Our

findings supported a different theory regarding the movement of crystals after a sonic ejection. By studying individual crystal movement in the 3D liquid we determined that crystals are ejected from surface layer. However, instead of drawing the new crystals from the bottom of the solution as was the commonly accepted theory, the surface layer instead “heals” the removed part primarily via a surface tension mechanism. Thus crystals are always drawn from the top layer, and once the top layer of the liquid is completely depleted the ejected drops begin to come from lower down. This finding can be visualized in the graph in Figure 10, and further details on the 3D imaging of crystal harvesting are discussed in by [12].

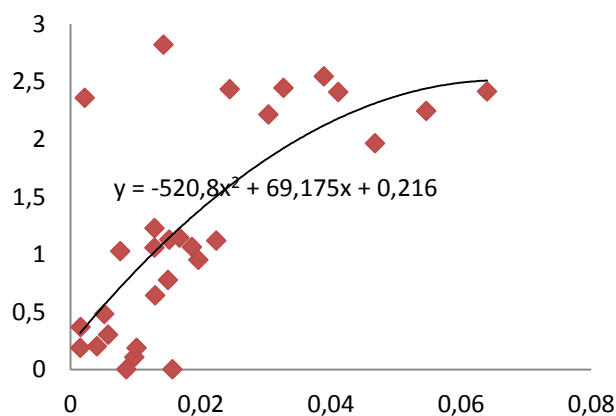


Figure 10: Crystal Movement (μm) vs. Crystal Depth (μm). In this figure, each point represents a crystal in the solution, the x axis represents the movement of the crystal between the before ejection stack and the after ejection stack, and the y axis represents the depth of the crystal in the drop. As we can see from the fitted line, we have a strong correlation showing that the upper level crystals are much more likely to move, and lower level crystals stay much more stationary. This supports the “healing” theory discussed previously.

CONCLUSION

This paper reports the progress on the enhancement of the on-axis microscope techniques used at synchrotron beamlines at NSLS-II. We have successfully explored Image Stacking that not only provides sharper images, but also provides depth and 3D information about samples. We successfully converted a weakness (shallow DoF) into a strength, by recovering 3rd depth dimension of images with single on-axis camera.

ACKNOWLEDGMENT

We acknowledge Alexei Soares for discussion and image collection of the biological crystals, Scott Coburn for engineering design, and Alexey Suvorov for optimization and image collection of the KB mirror system at 10-ID.

Work at Brookhaven was supported by the Department of Energy, Office of Basic Energy Sciences, under contract DE-SC0012704

APPENDIX

Due to limitations of the printed version, all videos obtained from Image Stacking are provided on the [www.youtube.com](https://www.youtube.com/channel/UC-SfBpwDIuw41_r0qqYkZQ) channel: 3D Microscope. The following is URL to the two 3D model videos on the channel https://www.youtube.com/channel/UC-SfBpwDIuw41_r0qqYkZQ [11].

REFERENCES

- [1] K. J. Gofron, Y. Q. Cai, D. S. Coburn, S. Antonelli, J. Flores, and A. Suvorov, “On-axis microscopes for the inelastic x-ray scattering beamline at NSLS-II”, AIP Conf. Proc. 1741, 030027 (2016); doi: 10.1063/1.4952850.
- [2] Gofron, K. J., Molitsky, M., “On axis sample visualization along a synchrotron photo beam”, U.S. Patent No. 8,440,986, May 14 2013.
- [3] K. J. Gofron and N. E. C. Duke, “Using X-ray excited UV fluorescence for biological crystal location”, Nucl. Instr. and Meth. A, 649, pp. 216-218 (2011).
- [4] M. R. Fuchs, D. K. Bhogadi, J. Jakoncic, S. Myers, R. M. Sweet, L. E. Berman, J. Skinner, M. Idir, O. Chubar, S. McSweeney, and D. K. Schneider, “NSLS-II biomedical beamlines for micro-crystallography, FMX, and for highly automated crystallography, AMX: New opportunities for advanced data collection”, AIP Conf. Proc. 1741, 030006, (2016); doi: 10.1063/1.4952829.
- [5] M. L. Rivers, “areaDetector: EPICS Software for 2-D Detectors” in *Proc. 16th Int. Conf. on Accelerator and Large Experimental Physics Control Systems, ICALEPCS’17, Barcelona, Spain, Oct. 2017*, paper THDPL03, this conference.
- [6] K. J. Gofron, and A. Joachimiak, “Visualization of X-ray Beam Using CdWO₄ Crystal for Macromolecular Crystallography”, J. Systemics Cybernetics and Informatics 9, No 6, pp. 87-93 (2011).
- [7] J. Wlodek, *et al.*, in preparation.
- [8] OpenCV Library, opencv.org/
- [9] M. Moeller, M. Benning, C. Schonlieb, and D. Cremers, “Variational Depth From Focus Reconstruction.” IEEE Transactions on Image Processing, 24, No. 12, pp. 5369–5378. (2015), doi:10.1109/tip.2015.2479469.
- [10] Group, Khronos, “The Industry’s Foundation for High Performance Graphics”, [OpenGL.org](http://www.opengl.org/), <http://www.opengl.org/>.
- [11] Beetle and a mineral 3D microscope videos: https://www.youtube.com/channel/UC-SfBpwDIuw41_r0qqYkZQ
<https://www.youtube.com/watch?v=FdpdAdoiRwA>,
<https://www.youtube.com/watch?v=UFx2EDou0-k>
- [12] Y. N. Samara, H. M. Brennan, L. McCarthy, M. T. Bollard, D. Laspina, J. M. Wlodek, S. L. Campos, R. Natarajan, K. J. Gofron, S. McSweeney, A. S. Soares, and L. Leroy, “Using sound pulses to solve the crystal harvesting bottleneck”, Acta Crystallographica D (2018), to be published.